DOI: 10.1002/chem.200500495

Synthesis and Luminescence Properties of Ag_2S and PbS Clusters in Zeolite A

Claudia Leiggener and Gion Calzaferri*[a]

Abstract: Zeolite A provides a suitable environment to host Ag_2S and PbS clusters, so that spectroscopic investigations on very small particles are possible. The Ag_2S monomer is colorless and shows photoluminescence at 490 nm with a lifetime of 300 μs, while the absorption and luminescence of Ag_4S_2 and larger clusters are red-shifted. The properties of these Ag_2S/zeolite A materials depend on the co-cations. Results for Li^+, Na^+, K^+, Rb^+, Cs^+, Mg^{2+}, Ca^{2+}, and Sr^{2+} are reported. Excitation energy transfer between Ag_2S and Ag_4S_2 has been studied in materials containing Ca^{2+} co-cations. PbS particles can be prepared by the same method as Ag_2S in the cavities of zeolite A. The PbS monomers obtained are yellow and show photoluminescence at 570 nm, with a lifetime of 700 ns.

Keywords: cluster compounds · host–guest systems · lead sulfide · luminescence · silver sulfide · zeolites

Introduction

Zeolites can act as protecting hosts for supramolecular organization of different kinds of atoms, ions, and molecules, which leads to host–guest materials with a large variety of challenging properties.[1] A common way to obtain zeolite guest systems is by means of a "ship-in-a-bottle" synthesis.[2] This name is due to artistic bottles containing a ship that is larger than the bottle neck. In chemistry it means the in situ synthesis of compounds occluded in a host material. This is done by inserting sufficiently small molecules and ions into the cavities of the host and allowing further reaction until the product is too large to leave the cavities. Transition-metal sulfides have been synthesized in different zeolite framework types. The zeolite prevents the small particles from growing or aggregating into large clusters or bulk materials. Small transition-metal sulfide particles show significantly changed optical properties due to the quantum-size effect.[3,4] Some of them have been discussed for catalytic applications.[5,6] The cavities of zeolite A provide an appropriate environment to host silver ions and small silver sulfide clusters. In previous publications we reported the synthesis and some properties of these host–guest materials.[7] We found that the smallest silver sulfide species that can be stabilized in the α-cages of zeolite A are the Ag_2S monomer and the Ag_4S_2 dimer. Both species show photoluminescence in the visible region, Ag_2S at 490 nm and Ag_4S_2 at 610 nm.[8] Luminescence properties strongly depend on temperature, while the luminescence of Ag_4S_2 shows stronger thermal quenching than the luminescence of Ag_2S. This results in a reversible color change of the total luminescence with temperature, and is illustrated in Figure 1 for crystals containing Ca^{2+} as co-cations. A single zeolite A crystal containing Ag_2S and Ag_4S_2 can therefore be regarded as a tiny luminescent thermometer.

The optical properties depend, to a certain extent, on the charge-compensating cations (co-cations) of the zeolite. In the presence of K^+ as co-cations a new phenomenon appears that is known as luminescence thermochromism. We observed that zeolite A samples containing K^+ and silver sulfide show, at room temperature, a bright deep-red photoluminescence with maximum emission at 730 nm, which is replaced by the luminescence of Ag_2S and Ag_4S_2 at low temperature.[9] These results suggest a specific interaction between K^+ and silver sulfide. The K^+ ion can also be added after the silver sulfide synthesis and the detection of the red luminescence is then a proof of the presence of potassium ions. In this paper we will discuss the influence of different co-cations. It will be shown that they influence the coordination sites of silver ions and also the luminescence properties of the final silver sulfide clusters. In samples containing

[a] Dr. C. Leiggener, Prof. Dr. G. Calzaferri
Department of Chemistry and Biochemistry
University of Bern
Freiestrasse 3, 3012 Bern (Switzerland)
Fax: (+41)-031-631-39-94
E-mail: gion.calzaferri@iac.unibe.ch

 © 2005 Wiley-VCH Verlag GmbH & Co. KGaA, Weinheim WILEY InterScience DISCOVER SOMETHING GREAT

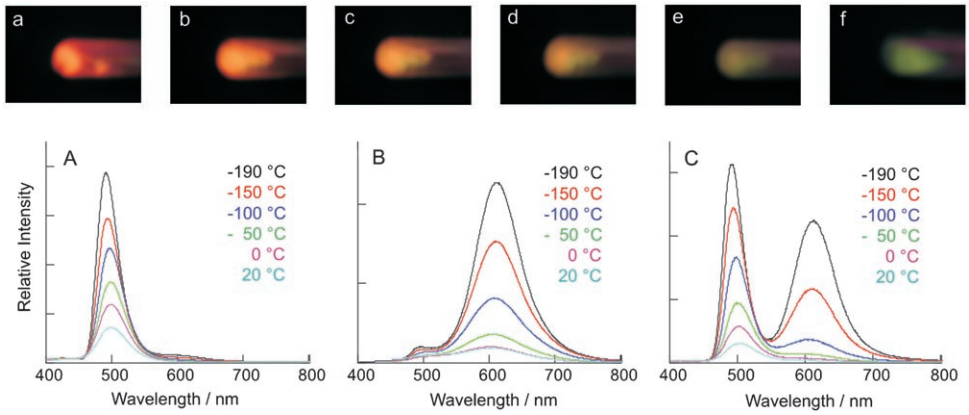

Figure 1. Top: photographic pictures of luminescent zeolite A hosting Ag_2S and Ag_4S_2, directly after cooling with liquid nitrogen (a), at increasing temperature (b–e), and at room temperature (f). Bottom: Temperature-dependent luminescence spectra of Ag_2S and Ag_4S_2 in zeolite A. A) Ag_2S, B) Ag_4S_2, and C) Ag_2S and Ag_4S_2.

Ag_2S and Ag_4S_2 energy transfer from excited Ag_2S to Ag_4S_2 occurs; this process will be exemplified for Ca^{2+}-exchanged zeolite A.

Lead sulfide clusters are well studied objects. PbS monomers have been stabilized in argon matrices, so that they could be investigated spectroscopically.[10] The lowest energy absorption band lies in the visible region at about 450 nm, while the luminescence is expected to be around 584 nm.[11] PbS clusters were obtained by loading zeolite Y with lead sulfide. This leads to yellow materials.[12] The color change of Pb^{2+}-exchanged zeolite Y from colorless to yellow upon exposure to H_2S, was attributed to the formation of PbS monomers. Larger PbS clusters have been synthesized by using different kinds of stabilizing agents, such as thiols,[13] reverse micelles,[14] trimethylsilane (TMS) sol–gel films,[16] and polymers.[17] The PbS clusters described in references. [13–16] all show photoluminescence in the near IR, and the emission wavelength can be tuned to the particle size, which lies in the nanometer range. We found that the same ship-in-a-bottle synthesis that has been successful for obtaining well-defined silver sulfide clusters in zeolite A also leads to well-defined PbS/zeolite A materials, and that these materials show photoluminescence in the visible region.

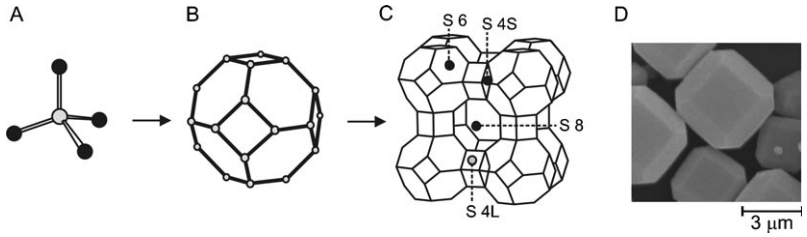

Figure 2. A scheme of the building units of zeolite A (A–C) and an SEM image of typical zeolite A crystals (D). C shows the framework of zeolite A with its crystallographically identified cation positions.

Results and Discussion

Ag^+ exchange in zeolite A: Ag^+-exchanged zeolite A is the starting material for the silver sulfide cluster synthesis. The synthesis procedure is based on the knowledge that Ag^+-exchanged zeolite A can be reversibly dehydrated (activated) at room temperature.[19] Under ambient conditions the cations are coordinated to water molecules that are also present inside the zeolite cages. The framework of zeolite A consists of alternating SiO_4 and AlO_4 tetrahedra. The tetrahedra are connected over the oxygen atoms in the corners, resulting in a larger building unit called a β-cage (or sodalite cage), which is illustrated in Figure 2. The oxygen bridges are represented as black lines and the dots stand for Si and Al atoms. Eight β-cages are linked together over the 4-rings giving rise to a larger cavity called an α-cage. The diameter of the α-cage is 11.4 Å, while the largest window (8-ring, see Figure 2C) has a diameter of 4.1 Å. In dehydrated zeolites the cations have three different possibilities for coordination to the oxygen atoms of the framework. Either they coordinate to a 4-ring (18 sites/α-cage), or to a 6-ring (eight sites/α-cage), or to an 8-ring (three sites/α-cage). In the case of the 4-ring one can distinguish between two possible positions, position S4S in the β- and position S4L in the α-cage. For small cations like Na^+ and Ca^{2+} the preferred position is S6 in the 6-ring. In one pseudo unit cell eight Na^+ ions are located at S6, three Na^+ ions at S8, and one Na^+ ion at S4L. In $Ca_6[(SiO_2)_{12}(AlO_2)_{12}]$ all six Ca^{2+} ions are coordinated to S6.[20]

Silver ions can be inserted into zeolite A by means of ion exchange. The silver loading (x) is adjusted by choosing different Ag^+ concentrations in solution. The loading denotes the number of silver ions per α-cage and has values between 0 and 12. For samples with different silver loadings the following abbreviation is used Ag_xM_yA, in which A stands for the framework of zeolite A, M for the co-cations, $y=12-x$ for monovalent co-cations, and $y=6-0.5x$ for divalent co-cations. All these samples are colorless in their fully hydrated form and their absorption spectra are similar to Ag^+ in water. In dehydrated silver zeolite A, however, Ag^+ is forced to coordinate to zeolite oxygen, because no other coordination options are present. This coordination leads to a change of the absorption properties of the material. In some

 © 2005 Wiley-VCH Verlag GmbH & Co. KGaA, Weinheim

cases a reversible color change from colorless to yellow upon dehydration is observed. The yellow color is due to Ag^+ coordinated to the 4-ring site, while 6-ring and 8-ring coordinated Ag^+ gives rise to transitions in the UV region.[19,21,22]

We studied the reversible color change as a function of the co-cations and of the silver loading. The results are summarized in Table 1. In the case of Na^+ co-cations the samples turn yellow at a very low silver loading ($x<0.2$), in every other case a silver loading $x>1$ is necessary. For Li^+ and K^+ co-cations a color change starts at $x=4$. These results show that in zeolite NaA the Na^+ ions that occupy the 4-ring positions are exchanged easier for Ag^+ than the Na^+ ions that occupy the 8- and 6-ring positions, while in other cation forms the exchange does not start with the 4-ring ion. These findings are consistent with results obtained from the evaluation of the ion-exchange data of Ag^+/Na^+ and Ag^+/K^+ exchange isotherms of zeolite A.[22] In $Rb_{10}Na_2A$ and Cs_6Na_6A, three Rb^+ and Cs^+ ions prefer to coordinate to the 8-ring sites due to their size and the others are expected to be at the 6-ring sites.[23] Upon exchange with silver we know that it is not the cation in the 4-ring position that is first exchanged, but rather the cations in the 6- and 8-ring positions.

Table 1. Ag_xM_yA; M^{n+} are the co-cations and x_{yellow} is the silver loading at which the samples turn yellow upon dehydration.

M^{n+}	Ca^{2+}	Na^+	K^+	Li^+	Rb^+/Na^+[a]	Cs^+/Na^+[b]
x_{yellow}	10[19]	<1[19]	>3	>3	>1	>1

[a] $Rb_{10}Na_2A$. [b] Cs_6Na_6A.

Silver sulfide clusters in zeolite A: Detailed studies on silver sulfide clusters in zeolite CaA showed that at low-to-medium silver loading ($x=0.01$–2) the formation of Ag_2S and Ag_4S_2 is favored, while at higher silver loading $(Ag_2S)_n$ clusters with $n=3$ or 4 are probably present. At a silver loading of 0.01 the samples contain only Ag_2S monomers (Figure 1A), while at a silver loading of 2 mainly Ag_4S_2 (Figure 1B) monomers exist. In between these limits the samples contain both species and the ratio of Ag_2S/Ag_4S_2 decreases with increasing silver loading. The rise of the luminescence band of Ag_4S_2 appears simultaneously with a decrease of the relative luminescence of Ag_2S. The relative luminescence intensities of Ag_2S and Ag_4S_2 in Ag_2S-CaA-x, as a function of the silver loading, are plotted in Figure 3. The relative luminescence intensities were calculated by using Equation (1) and (2), in which I_{490} is the luminescence intensity at 490 nm (Ag_2S), and I_{610} is the luminescence intensity at 610 nm (Ag_4S_2).

$$I_{(Ag2S)} = \frac{I_{490}}{I_{490} + I_{610}} \quad (1)$$

$$I_{(Ag4S2)} = \frac{I_{610}}{I_{490} + I_{610}} \quad (2)$$

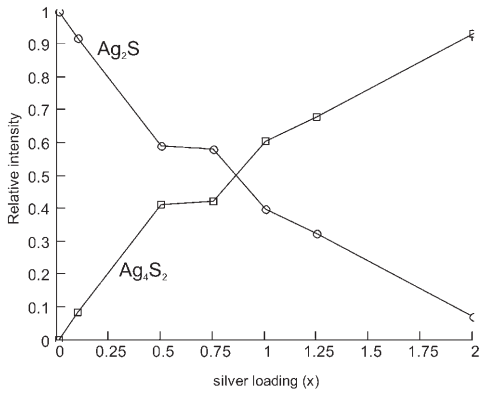

Figure 3. A plot of the relative luminescence intensities of Ag_2S and Ag_4S_2 in zeolite CaA as a function of the silver loading (x).

Influence of the co-cations: The co-cations influence the nearest environment of the silver sulfide clusters inside the zeolite cages. Depending on the co-cations, the amount of water, the availability of coordination sites, and the pore size (opening of the 8-ring) of the zeolite differ. In a series of experiments silver sulfide clusters were synthesized in different cation forms of zeolite A. The cations were alkali and alkaline-earth cations, namely Li^+, Na^+, K^+, Rb^+, Cs^+, Mg^{2+}, Ca^{2+}, and Sr^{2+}, which can be introduced by means of ion exchange before the silver sulfide cluster synthesis. It was expected that, within the defined silver loading range of 0.1–2, Ag_2S and Ag_4S_2 particles could be synthesized similar to those observed in CaA. In general, samples with a low silver loading are colorless and become more and more colored with increasing silver loading. They usually show an intense photoluminescence at low temperature, which is in some cases also intense at room temperature. Exceptions are Ag_2S-RbNaA and Ag_2S-CsNaA samples, which show no or only very weak photoluminescence. Figure 4 illustrates the temperature-dependent luminescence spectra of samples with similar silver loading (0.5–1) and different co-cations. One can roughly distinguish between three types of spectra. Type 1: spectra of samples containing divalent cations (A, B, and C) consisting of two emission bands. Considering the excitation spectra these two bands can be assigned to Ag_2S and Ag_4S_2. Type 2: spectra of samples containing Li^+ and Na^+ (D and E) consisting of three emission bands. The most significant difference of type 2 spectra compared to spectra of type 1 is the additional band at 540 nm. From phenomenological reasoning one can assume that it is due to Ag_2S monomers at a less-favorable site in the zeolite, and that it only appears if there are no other sites available. An example for such a less-favorable site is a position near the 4-ring. In the following text, the two different Ag_2S species are named $Ag_2S(480)$ and $Ag_2S(540)$, relating to their emission wavelength. The luminescence lifetimes of $Ag_2S(480)$ and $Ag_2S(540)$ in Ag_2S-LiA-1 are similar at $-160\,°C$ (see

 © 2005 Wiley-VCH Verlag GmbH & Co. KGaA, Weinheim

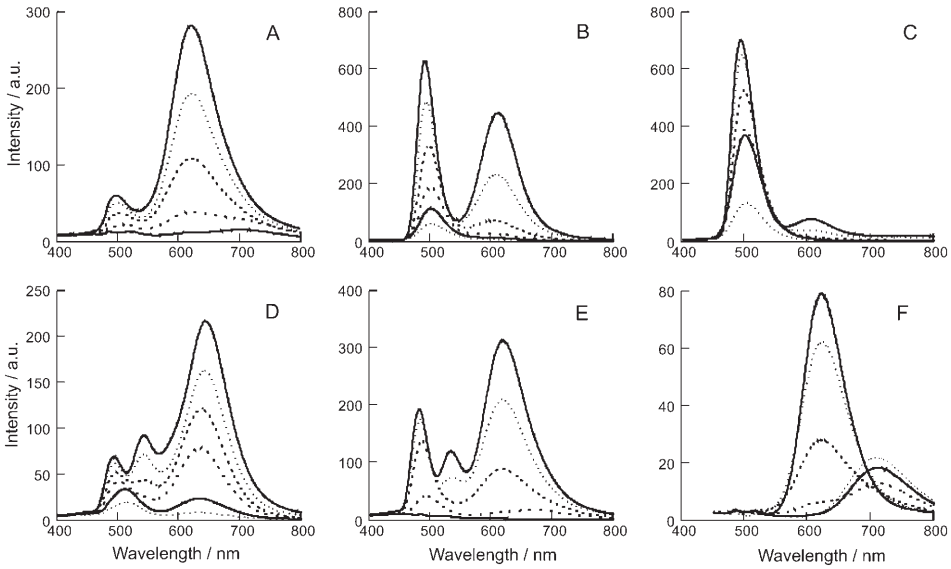

Figure 4. Luminescence spectra of Ag_2S-MA-x at different temperatures (−190, −150, −100, −90, and 0 °C, showing the decreasing intensity of bands (A–E), respectively, and of the short-wavelength band (F) at 20 °C upon excitation at 320 nm are shown. A: Ag_2S-MgA-1, B: Ag_2S-CaA-0.75, C: Ag_2S-SrA-1, D: Ag_2S-LiA-1, E: Ag_2S-NaA-0.5, and F: Ag_2S-KA-1.

Table 2). The luminescence decay has to be fitted to a three-exponential function in both cases. It would be interesting to investigate the role of $Ag_2S(540)$ in energy-transfer processes between Ag_2S and Ag_4S_2. Type 3: spectra of samples

Table 2. Luminescence lifetimes τ_n in μs and the corresponding amplitudes (a_n) of Ag_2S-LiA-1 at −160 °C after excitation at 320 nm. $\langle\tau\rangle$ is the average luminescence lifetime in μs.

λ_{em} [nm]	τ_1 (a_1)	τ_2 (a_2)	τ_3 (a_3)	$\langle\tau\rangle$
480	406 (0.032)	129 (0.150)	6 (0.818)	208
540	506 (0.030)	135 (0.181)	6 (0.789)	247

containing K^+ show an additional emission band at elevated temperature, not observed in samples with other co-cations. All Ag_2S-KA-x samples ($0.1 \le x \le 2$) reveal a luminescence band at 730 nm, which is strongest at room temperature and becomes weaker with decreasing temperature until it disappears completely. The disappearance of this luminescence occurs simultaneously with a rise of the luminescence bands of Ag_2S and Ag_4S_2. This phenomenon is reversible and is known as luminescence thermochromism.[9]

Although the reasons for these three types of spectra are not obvious, it is nevertheless interesting that the luminescence of the samples can be changed by exchanging the cations. It is also possible to exchange the co-cations after the silver sulfide synthesis if the silver sulfide content is not too high.[9] So, one may wonder if these materials could be used for detecting specific cations. In general, one could also try to exchange the co-cations with any other cations. A strong effect is observed when Ag_2S-CaA-x is suspended in an aqueous solution containing silver ions. A yellow sample (e.g., Ag_2S-CaA-1) turns orange within seconds. This indicates a very fast exchange of cations from the inside of the zeolite (Ca^{2+} and H^+) with Ag^+ ions from solution and a strong electronic interaction between Ag^+ and silver sulfide. The color change is shown in the spectra in Figure 5. The difference spectrum demonstrates that there are new transitions at 480 nm and in the UV region, due to the additional Ag^+ ions. These transitions are not observed in pure Ag^+-CaA and can therefore be assigned to $Ag^+(Ag_2S)_n$ clusters.

Energy transfer between Ag_2S and Ag_4S_2: The luminescence lifetimes of silver sulfide clusters in zeolite A all lie in the microsecond timescale. They were studied as a function of the silver loading and of temperature. The longest luminescence lifetime in Ag_2S-CaA-x are observed in isolated Ag_2S molecules, with a lifetime of about 300 μs. The luminescence decay of Ag_2S can be fitted to a single-exponential function. However, as soon as Ag_4S_2 clusters are present in the same zeolite crystal the decay is no longer single exponential. It can then be fitted to a bi-exponential function, and the average luminescence lifetime was found to decrease with an increasing amount of Ag_4S_2. The data from a series of measurements of samples containing different ratios of Ag_2S and Ag_4S_2 are summarized in Table 1 of reference [8]. The explanation given there is that energy transfer from excited Ag_2S to Ag_4S_2 occurs. Actually, we have a similar situation as described by Förster[24] in which the donor and the acceptor molecules are treated to be at fixed positions. In our case the donors are Ag_2S and the acceptors are Ag_4S_2 and are spatially separated from each other by the zeolite framework, as illustrated in Figure 6. The rate constant for energy transfer k_{EnT} strongly depends on the distance between the donor and acceptor, and can be expressed by Equation (3), in which τ_{D^*} is the luminescence lifetime of the donor without acceptor, R_0 is the Förster radius, and R_i is the distance between the donor and acceptor.

$$k_{EnT}(i) = \frac{1}{\tau_D}\left(\frac{R_0}{R_i}\right)^6 \qquad (3)$$

With increasing donor–acceptor distance the probability of radiative relaxation of the donor increases. In the situation shown in Figure 6 the probability of the excitation energy of Ag_2S being transferred to the nearest Ag_4S_2 (distance R_1) is therefore much higher than to the diagonal lying Ag_4S_2 (distance R_2).

 © 2005 Wiley-VCH Verlag GmbH & Co. KGaA, Weinheim

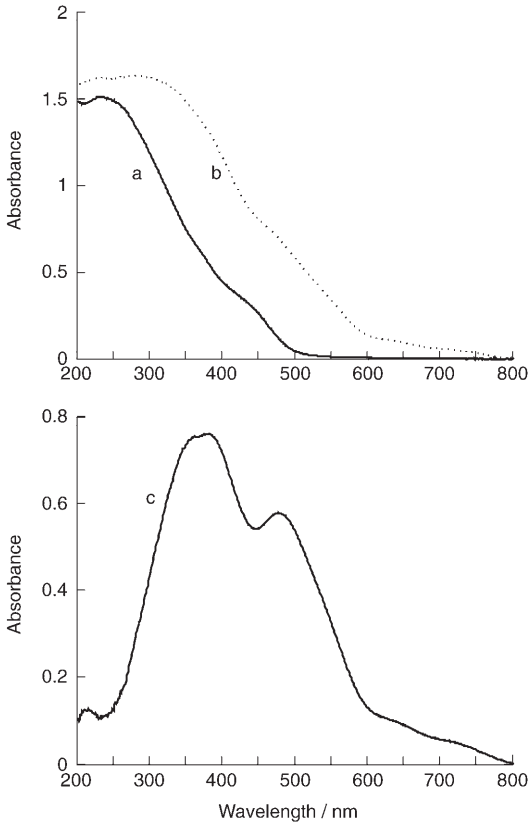

Figure 5. Diffuse reflectance spectrum of a) Ag_2S-CaA-1 and b) Ag^+/Ag_2S-CaA-1. c) Difference spectrum of Ag_2S-CaA-1 and Ag^+/Ag_2S-CaA-1.

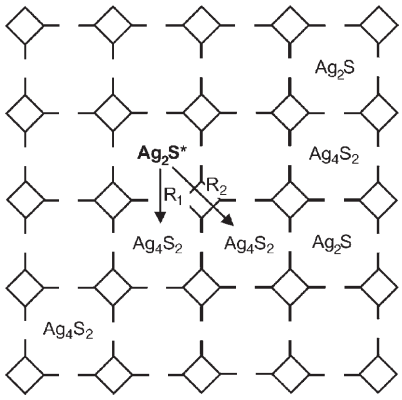

Figure 6. Scheme of Ag_2S and Ag_4S_2 in the α-cages of a zeolite A crystal. An excited Ag_2S can transfer its excitation energy to a neighboring Ag_4S_2.

The luminescence decay of the donor can then be described by a stretched exponential function, because the donors and acceptors are randomly distributed in the host. This is shown in Equation (4), in which ρ_{D^*} is the luminescence intensity of the donor as a function of time and γ is a parameter, which is expected to be proportional to the concentration of acceptors.[24]

$$\langle \rho_{D*}(t) \rangle = exp\left(-\frac{t}{\tau_{D*}}\right) \cdot \exp\left(-2\gamma\sqrt{\frac{t}{\tau_{D*}}}\right) \quad (4)$$

We studied a series of samples with different silver loading and thus different amounts of Ag_2S and Ag_4S_2. As an example the time-resolved luminescence spectra of Ag_2S-CaA-0.5 are shown in Figure 7. The luminescence decay of Ag_2S at 490 nm was fitted to Equation (4). The values of γ and τ, as a function of the silver loading, are listed in Table 3.

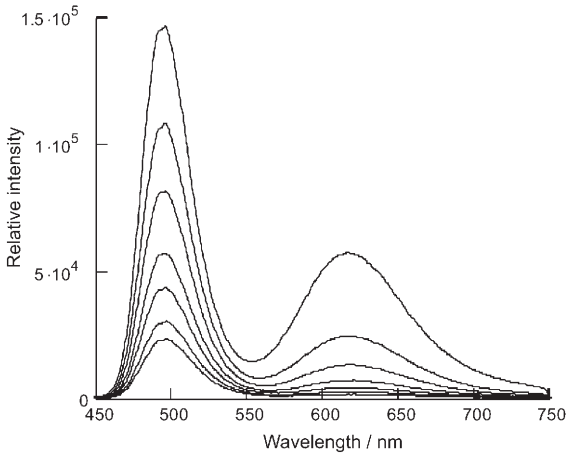

Figure 7. Time-resolved luminescence spectra of Ag_2S-CaA-0.5 at −150 °C. The first six spectra after the excitation pulse are shown. Excitation was performed at 320 nm and the time window for detection (gate) was 100 μs.

Table 3. Values of γ and τ for the luminescence decay of Ag_2S in Ag_2S-CaA-x as a function of the silver loading (x). The values are mean values from three independent measurements.

x[Ag^+/α-cage]	γ	τ [μs]
0.1	0.064	277
0.5	0.125	211
0.75	0.126	253
1.0	0.203	169
1.25	0.227	197

The value of γ increases with increasing silver loading. This corresponds to what we expected, because with increasing silver loading the concentration of acceptors (Ag_4S_2) increases, and hence γ is expected to become larger. Another factor which may favor energy transfer at higher silver loadings is the decreasing average distance between the donor and acceptor, due to an increasing total concentration of silver sulfide clusters with increasing silver loading.

Lead sulfide clusters in zeolite A: Zeolites NaA and CaA were loaded with one Pb^{2+} ion per α-cage. After the Pb^{2+} exchange and dehydration in high vacuum, the zeolite samples were still colorless. As an example, the absorption spectrum of Pb^{2+}-zeolite A is shown in Figure 8. Upon exposure to H_2S gas the color changes to yellow. This is consistent with what has been observed for zeolites L and Y. Moller

 © 2005 Wiley-VCH Verlag GmbH & Co. KGaA, Weinheim

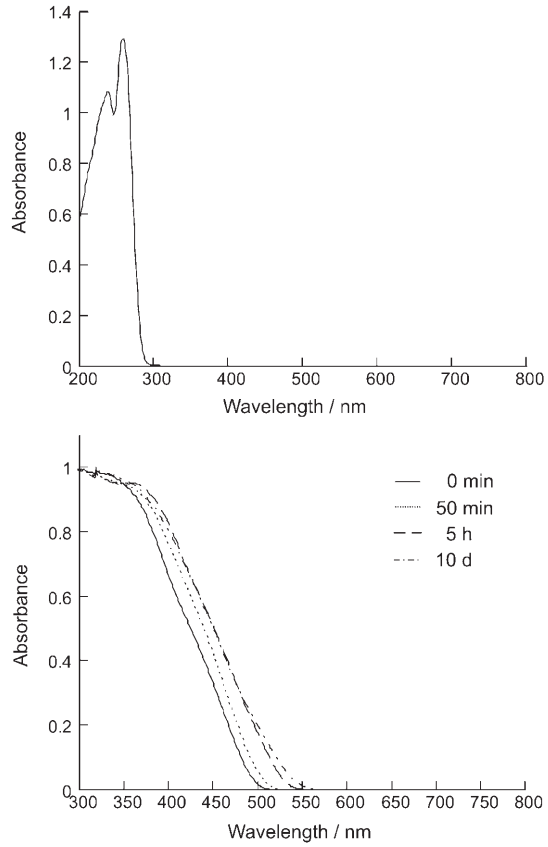

Figure 8. Top: Diffuse reflectance spectrum of Pb^{2+} zeolite A. Bottom: Diffuse reflectance spectra, scaled to the same height, of PbS-NaA-1 in a quartz vessel at different times after rehydration. The spectra were converted into absorption spectra by applying the Kubelka–Munk function.

et al. suggest that this color change is due to the formation of PbS monomers,[12] according to Equation (5).

$$Pb_{(zeolite)}{}^{2+} + H_2S_{(g)} \rightarrow PbS_{(zeolite)} + 2\,H_{(zeolite)}{}^{+} \qquad (5)$$

So, in a sample with a lead loading of 1, two protons per α-cage are created. This should not affect the stability of the zeolite much under the applied conditions, but it could be problematic for higher lead loadings, for which consecutive loading steps with an exchange of H^+ for other co-cations between the steps is recommended; this procedure is easy to realize.

The yellow color of PbS-NaA-1 and PbS-CaA-1 becomes stronger and more orange with time after rehydration. The absorption spectra in Figure 8 illustrate that the absorption edge shifts to longer wavelengths within the first few hours after rehydration, but after some time the changes are not so significant. These samples show a yellow-orange photoluminescence upon cooling with liquid nitrogen. The luminescence and the excitation spectra of PbS-NaA-1 are shown in Figure 9. The luminescence decay can be fitted to a bi-exponential function with an average luminescence lifetime around 700 ns. The parameters of the luminescence decay at maximum emission (568 nm) are shown in Table 4.

Table 4. Luminescence lifetimes (τ_n) in ns and the corresponding amplitudes (a_n) at the emission maximum (568 nm) of PbS-NaA-1 at −160 °C.

τ_1 [ns]	a_1	τ_2 [ns]	a_2	$\langle\tau\rangle$ [ns]
156	0.717	961	0.283	727

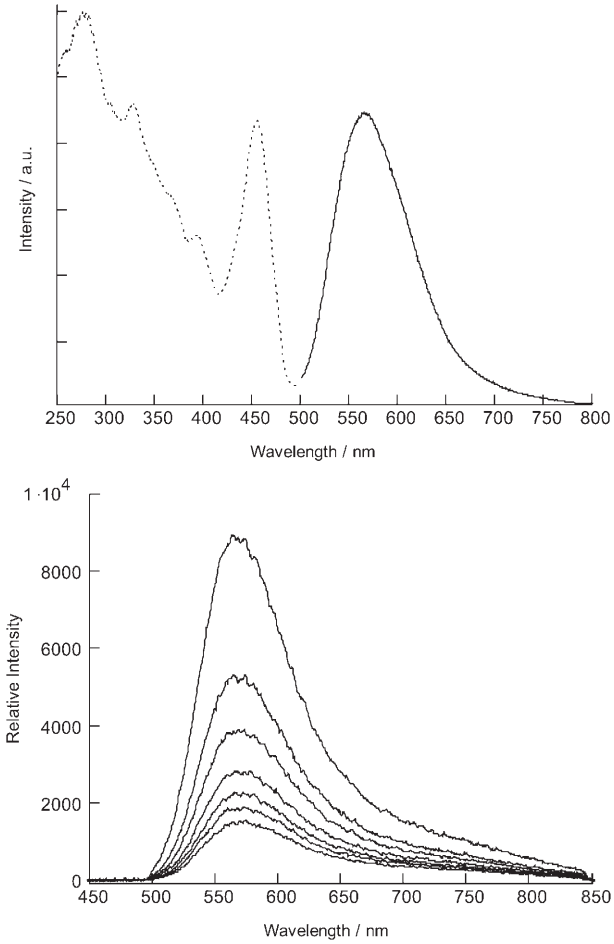

Figure 9. Top: Luminescence (solid line) and excitation (dots) spectra of PbS-NaA-1 at −190 °C. Bottom: Time-resolved luminescence spectra of the same sample at −160 °C. The first seven spectra after the excitation pulse are shown. Excitation was performed at 440 nm and the time window for detection (gate) was 500 ns.

The luminescence maximum at 568 nm fits quite well to the energy of the HOMO–LUMO transition of a calculated PbS monomer[11] and the excitation spectrum corresponds well to the absorption spectrum of molecular PbS in argon matrices.[10] So, we can say that after rehydration of PbS-NaA-1 there is still a large amount of PbS monomer in the zeolite. However, the red shift of the absorption edge after rehydration lets us assume that in a zeolite A, cluster growth takes place similar to that observed for silver sulfide clusters, and that the final lead sulfide clusters stay inside the α-cages of zeolite A. Therefore, in the hydrated samples there are probably some larger clusters, such as Pb_2S_2. This

 © 2005 Wiley-VCH Verlag GmbH & Co. KGaA, Weinheim

could be an explanation for the bi-exponential luminescence decay and the long-wavelength component in the time-resolved luminescence spectra.

Our yellow samples contrast with the colorless PbS–zeolite A materials,[25] which have been synthesized in a different way. Our results, as well as the results reported in references [10–12] do not correspond to those published in reference[25]. Since the PbS monomer already absorbs in the visible region, it is not possible to synthesize colorless PbS clusters, and one has to doubt if the authors really obtained lead sulfide particles with the stoichiometry they have assumed.

Conclusion

We have shown that zeolite A is a versatile host for the ship-in-a-bottle synthesis of silver sulfide and lead sulfide clusters. These host–guest materials are stable under ambient conditions and show a variety of interesting luminescence properties. The luminescence decay of the Ag_2S monomer can be described by a stretched-exponential function. This confirms the interpretation of excitation energy transfer between Ag_2S and Ag_4S_2 in zeolite A crystals. By studying the influence of the co-cations on the optical properties of Ag_2S/zeolite A materials, we observed a clear change in the sample color upon addition of silver ions, suggesting the formation of new silver-rich cluster species. The same synthesis procedure as for silver sulfide clusters was successfully applied to obtain lead sulfide clusters in zeolite A. A lead loading of one Pb^{2+} per α-cage yields yellow PbS/zeolite A guest–host materials. In contrast to what has been observed in other zeolites, the lead sulfide clusters are also stable in hydrated zeolite A. The hydrated PbS/zeolite A samples show photoluminescence in the visible region at 570 nm, which is a new observation, and which is most probably due to PbS monomers. Our findings are in contradiction with data reported in reference [25], which we consider to be erroneous.

Experimental Section

Synthesis: Zeolite A ($Na_{12}[(SiO_2)_{12}(AlO_2)_{12}]\cdot 27\,H_2O$) was synthesized and characterized according to the literature[18] The ion-exchanged forms were obtained by suspending zeolite NaA (500 mg) in an aqueous $M(NO_3)_n$ solution (0.5 M, 20 mL) ($M^{n+}=Li^+$, K^+, Rb^+, Cs^+, Mg^{2+}, Ca^{2+}, Sr^{2+}) for 15 min. This step was repeated twice and the samples were washed three times with doubly distilled water. The ion-exchanged samples were analyzed by means of energy-dispersive X-ray analysis (EDX) and thermogravimetric analysis (TGA). For most cases fully exchanged samples were obtained except for Rb^+ and Cs^+, for which the following compositions were found: $Rb_{10}Na_2[(SiO_2)_{12}(AlO_2)_{12}]\cdot 23\,H_2O$ and $Cs_6Na_6[(SiO_2)_{12}(AlO_2)_{12}]\cdot 20\,H_2O$. The silver sulfide clusters were synthesized according to references [7,8]. The following abbreviations are used: Ag_xM_yA for partially silver-exchanged zeolite A, in which A stands for the framework of zeolite A and M stands for the co-cations ($y=12-x$ for monovalent co-cations and $y=6-0.5x$ for divalent co-cations); and Ag_2S-MA-x for zeolite A containing silver sulfide clusters, in which x denotes the silver loading (number of Ag^+ per α-cage). For the lead sulfide cluster synthesis, zeolite NaA (100 mg) was suspended in an aqueous solution of $NaNO_3$ (10 mL, 0.01 M) and an aqueous solution of $Pb(NO_3)_2$ or $Pb(CH_3COO)_2$ (460 μL, 0.1 M) was added, leading to a lead loading of one Pb^{2+} ion per α-cage. The suspension was stirred for 3 h at room temperature and washed twice with doubly distilled water (15 mL). The samples were dried in high vacuum (10^{-6} mbar) at room temperature for 3 days, then they were exposed to 60 Torr of H_2S gas for 1 h. Upon exposure to H_2S a color change from colorless to yellow was observed. After removal of excess H_2S, the samples were rehydrated in air. Using the same nomenclature as for the silver sulfide samples, the final material was called PbS-NaA-1. The same procedure was used for synthesizing PbS clusters in zeolite CaA.

Spectroscopy: Diffuse reflectance spectra were recorded on a Perkin–Elmer Lambda 900 (UV/VIS/NIR) spectrophotometer with an integrating sphere and were converted into absorption spectra, by applying the Kubelka–Munk function. Steady-state luminescence spectra were recorded on a Perkin–Elmer LS 50B luminescence spectrometer equipped with an Oxford PE1704 cryostat and a thermostat, which allows measurements at temperatures between −195 °C (liquid nitrogen) and room temperature. Time-resolved luminescence measurements were performed by exciting the samples with a pulsed laser. The system used for this purpose consisted of a Nd:YAG laser (Quantel Brilliant), an OPO (Opotek MagicPrism Vibrant Vis) which was pumped by the third harmonic and an UV-Mixer Module for excitation in the UV. The energy of the laser pulse was around 4 mJ for visible light and 0.5 mJ for UV light, on a surface of about 0.5 cm^2. To determine the luminescence-decay curves, the time-dependent spectra were integrated over the wavelength region of interest.

Acknowledgements

This work was supported by the Swiss National Science Foundation, project NF 200020–105140.

[1] a) *Host–Guest Systems Based on Nanoporous Crystals*, (Eds.: F. Laeri, F. Schüth, U. Simon, M. Wark, VCH, Weinheim (Germany), **2003**. b) L. Tosheva, V. P. Valtchev, *Chem. Mater.* **2005**, *17*, 2494–2513.
[2] a) G. Meyer, D. Wöhrle, M. Mohl, G. Schulz-Ekloff, *Zeolites* **1984**, *4*, 30–34; b) D. Sendor, U. Kynast, *Adv. Mater.* **2002**, *14*, 1570–1574; c) A. Fukuoka, N. Higashimoto, Y. Sakamoto, M. Sasaki, N. Sugimoto, S. Inagaki, Y. Fukushima, M. Ichikawa, *Catal. Today* **2001**, *66*, 21–29; d) A. Corma, H. Garcia, *Eur. J. Inorg. Chem.* **2004**, 1143–1164.
[3] Y. Wang, N. Herron, *J. Phys. Chem.* **1987**, *91*, 257–260.
[4] F. Iacomi, *Surf. Sci.* **2003**, *532–535*, 816–821.
[5] E. J. M. Hensen, J. A. R. van Veen, *Catal. Today* **2003**, *86*, 87–109.
[6] R. W. Joyner, M. Stockenhuber, O. P. Tkachenko, *Catal. Lett.* **2003**, *85*, 193–197.
[7] a) D. Brühwiler, R. Seifert, G. Calzaferri, *J. Phys. Chem. B* **1999**, *103*, 6397–6399; b) D. Brühwiler, C. Leiggener, S. Glaus, G. Calzaferri, *J. Phys. Chem. B* **2002**, *106*, 3770–3777.
[8] C. Leiggener, D. Brühwiler, G. Calzaferri, *J. Mater. Chem.*, **2003**, *13*, 1969–1977.
[9] C. Leiggener, G. Calzaferri, *ChemPhysChem* **2004**, *5*, 1593–1596.
[10] a) Y. Wang, A. Suna, W. Mahler, R. Kasowski, *J. Chem. Phys.* **1987**, *87*, 7315–7322; b) R. A. Teichmann, E. R. Nixon, *J. Mol. Spectrosc.* **1975**, *54*, 78–86.
[11] C. Y. Yang, S. Rabii, *J. Chem. Phys.* **1978**, *69*, 2497–2499.
[12] K. Moller, T. Bein, N. Herron, W. Mahler, Y. Wang, *Inorg. Chem.* **1989**, *28*, 2914–2919.
[13] L. Bakueva, I. Gorelikov, S. Musikhin, X. S. Zhao, E. H. Sargent, E. Kumacheva, *Adv. Mater.* **2004**, *16*, 926–929.
[14] S. W. Buckner, R. L. Konold, P. A. Jelliss, *Chem. Phys. Lett.* **2004**, *394*, 400–404.
[15] M. A. Hines, G. D. Scholes, *Adv. Mater.* **2003**, *15*, 1844–1849.

 © 2005 Wiley-VCH Verlag GmbH & Co. KGaA, Weinheim

[16] A. Martucci, J. Fick, S.-E. LeBlanc, M. LoCascio, A. Haché, *J. Non-Cryst. Solids* **2004**, *345/346*, 639–642.
[17] a) E. Lifshitz, M. Sirota, H. Porteanu, *J. Cryst. Growth* **1999**, *196*, 126–134; b) M. Brumer, A. Kigel, L. Amirav, A. Sashchiuk, O. Solomesch, N. Tessler, E. Lifshitz, *Adv. Funct. Mater.* **2005**, 15, 1111–1116.
[18] P. Lainé, R. Seifert, R. Giovanoli, G. Calzaferri, *New J. Chem.* **1997**, *21*, 453–460.
[19] a) R. Seifert, A. Kunzmann, G. Calzaferri, *Angew. Chem.* **1998**, *110*, 1603–1606; *Angew. Chem. Int. Ed.* **1998**, *37*, 1521–1524; b) R. Seifert, R. Rytz, G. Calzaferri, *J. Phys. Chem. A* **2000**, *104*, 7473–7483.
[20] D. W. Breck, *Zeolite Molecular Sieves*, Wiley, NY, **1974** pp. 83–92, pp. 530–540.
[21] G. Calzaferri, C. Leiggener, S. Glaus, D. Schürch, K. Kuge, *Chem. Soc. Rev.* **2003**, *32*, 29–37.
[22] M. Meyer, C. Leiggener, G. Calzaferri, *ChemPhysChem* **2005**, *6*, 1071–1080.
[23] F. M. Higgins, G. W. Watson, S. C. Parker, *J. Phys. Chem. B* **1997**, *101*, 9964–9972.
[24] a) T. Förster, *Z. Naturforsch. A* **1949**, *4*, 321–327; b) T. Förster, *Fluoreszenz Organischer Verbindungen*, Vandenboeck & Ruprecht, Göttingen (Germany), **1951**.
[25] M. Flores-Acosta, M. Sotelo-Lerma, H. Arizpe-Chavez, F. F. Castillon-Barraza, R. Ramirez-Bon, *Solid State Commun.* **2003**, *128*, 407–411.

Received: May 3, 2005
Published online: September 29, 2005

 © 2005 Wiley-VCH Verlag GmbH & Co. KGaA, Weinheim